Veterinary Pathology
1-9

DOI: 10.1177/0300985817705176
journals.sagepub.com/home/vet

Ranid Herpesvirus 3 and Proliferative Dermatitis in Free-Ranging Wild Common Frogs *(Rana Temporaria)*

F. C. Origgi[1,2], B. R. Schmidt[3], P. Lohmann[4], P. Otten[5], E. Akdesir[1], V. Gaschen[6], L. Aguilar-Bultet[2], T. Wahli[1], U. Sattler[1], and M. H. Stoffel[6]

Abstract

Amphibian pathogens are of current interest as contributors to the global decline of amphibians. However, compared with chytrid fungi and ranaviruses, herpesviruses have received relatively little attention. Two ranid herpesviruses have been described: namely, *Ranid herpesvirus 1* (RHV1) and *Ranid herpesvirus 2* (RHV2). This article describes the discovery and partial characterization of a novel virus tentatively named *Ranid herpesvirus 3* (RHV3), a candidate member of the genus *Batrachovirus* in the family *Alloherpesviridae*. RHV3 infection in wild common frogs *(Rana temporaria)* was associated with severe multifocal epidermal hyperplasia, dermal edema, a minor inflammatory response, and variable mucous gland degeneration. Intranuclear inclusions were numerous in the affected epidermis together with unique extracellular aggregates of herpesvirus-like particles. The RHV3-associated skin disease has features similar to those of a condition recognized in European frogs for the last 20 years and whose cause has remained elusive. The genome of RHV3 shares most of the features of the *Alloherpesviruses*. The characterization of this presumptive pathogen may be of value for amphibian conservation and for a better understanding of the biology of *Alloherpesviruses*.

Keywords

Ranid herpesvirus 3, amphibians, frogs, skin, pathology, *Alloherpesviruses*, wildlife

Amphibians are undergoing an unprecedented decline worldwide, making them the most endangered class of vertebrates on the planet; at least a third of the species are listed as threatened (IUCN Red List), resulting in a major loss of biodiversity.[6] The causes of this decline have been reported to include habitat loss and destruction, pollution, and global warming.[7] More recently, diseases have also surfaced as relevant factors contributing to the global amphibian decline.[10,13] Pathogens that have been shown to play a primary role in the extinction of amphibian populations include the fungal agent *Batrachochytrium dendrobatidis*, which is responsible for amphibian mass mortality, local extirpation of populations, and even the extinction of species.[4,18,31] Similarly, a novel chytrid fungus, *Batrachochytrium salamandrivorans*, recently has been shown to cause major die-offs in populations of fire salamanders *(Salamandra salamandra)*, leading them to the brink of extinction in the affected geographical regions.[21] Together with fungi, viruses have also recently attracted attention as significant amphibian pathogens. In particular, viruses of the genus *Ranavirus* in the family *Iridoviridae* are threatening amphibians in several countries.[13] Ranavirus has been implicated in the decline of the common frog *(Rana temporaria)* in the UK[34] and the collapse of other amphibian populations in many nations.[27]

Despite numerous investigations, the number of causative agents is still relatively small and it is likely that several other unrecognized pathogens might be present in wild amphibian populations.[13,14] The reasons for this are diverse. They include (1) the difficulties in detecting affected amphibians in the wild in the absence of mass die-offs and (2) the limited availability of carcasses due to the relatively short time needed for them to be scavenged or to decompose in the wild.

[1]Department of Infectious Diseases and Pathobiology (DIP), Centre for Fish and Wildlife Health (FIWI), University of Bern, Bern, Switzerland
[2]Institute of Veterinary Bacteriology, DIP, Bern, Switzerland
[3]KARCH, Neuchâtel, Switzerland, and Department of Evolutionary Biology and Environmental Studies, University of Zurich, Zurich, Switzerland
[4]Veterinarian, Forch, Switzerland
[5]Fasteris SA, Geneva, Switzerland
[6]Division of Veterinary Anatomy, University of Bern, Bern, Switzerland

Supplemental material for this article is available on the *Veterinary Pathology* website at http://journals.sagepub.com/doi/suppl/10.1177/0300985817705176.

Corresponding Author:
F. C. Origgi, Department of Infectious Diseases and Pathobiology (DIP), Centre for Fish and Wildlife Health (FIWI), University of Bern, Länggassstrasse 122, 3001 Bern, Switzerland.
Email: francesco.origgi@vetsuisse.unibe.ch

In the early spring of 2015, we diagnosed a proliferative skin disease occurring in free-ranging common frogs *(R. temporaria)* associated with the presence of intralesional microorganisms with ultrastructural and molecular features consistent with a herpesvirus. Until now, 2 herpesviruses have been described in frogs, namely *Ranid herpesviruses* 1 and 2 (RHV1 and RHV2),[11,19,20,22,29] which belong to the family *Alloherpesviridae* in the order *Herpesvirales*. The genomes of RHV1 and RHV2 have been sequenced and are 220 to 240 Kb.[11] RHV1, also known as Lucke's renal adenocarcinoma-associated herpesvirus, was discovered in the first half of the 20th century and was shown to be associated with the development of renal adenocarcinomas in Northern leopard frogs *(Lithobates pipiens)*.[19,20] Furthermore, biology of RHV1 and of the associated tumors was reported to be temperature-dependent, with low temperatures being associated with viral replication and formation of inclusions, whereas at high temperature tumors would be devoid of viral inclusions and prone to metastasize.[5,22,23] RHV2 was isolated from the urine of tumor-bearing frogs.[29] There have been no documented outbreaks or diseases associated with RHV2 infection except for the occurrence of massive edema in frogs that had been exposed to the virus as tadpoles.[22,28] In addition to RHV1 and RHV2, skin diseases associated with uncharacterized herpesviruses were reported in *Rana dalmatina* in Italy and in Switzerland,[3,15] in the common frog in the UK,[30] and in the common spadefoot *(Pelobates fuscus)*, common frog, and *Rana arvalis* in Germany.[24]

The study presented here aimed to provide an initial characterization of RHV3 and of its associated pathology and pathogenesis combining genomic and morphological data in the attempt to better understand the biology of *Alloherpesviridae* and amphibian disease ecology and conservation.

Material and Methods

Animals

In late March 2015, common frogs *(R. temporaria)* were observed with obvious skin changes in a pond near Zurich, Switzerland. Two of the observed frogs were collected and brought to the Centre for Fish and Wildlife Health (FIWI) of the University of Bern, Switzerland, for further investigation. The frogs were euthanatized with an overdose of MS222 (permit number 66/2014 released by the Veterinäramt des Kantons Zürich).

Pathologic Examination

The 2 frogs underwent full necropsy; tissue samples from all the organs were collected in 10% buffered formalin, and 5-µm-thick sections were routinely prepared and stained with hematoxylin and eosin (HE). Special stains including periodic acid–Schiff (PAS), Grocott, Gram, and Giemsa were carried out according to standard protocols as needed.

Skin, liver, and kidney were fixed in 2.5% glutaraldehyde. Samples of affected skin were fixed for 1 to 2 days in 2.5% glutaraldehyde (Merck and Cie, Schaffhausen, Switzerland) in 0.1 M cacodylate buffer (Merck and Cie), pH 7.4, and postfixed with 1% OsO4 (Chemie Brunschwig, Basel, Switzerland) in 0.1 M cacodylate buffer, pH 7.4, for 2 hours at room temperature. Samples were then dehydrated in an ascending ethanol series and embedded in Epon (FLUKA, Buchs, Switzerland). The resin was polymerized for 5 days at 60°C. Semi-thin sections of 0.5 µm in thickness were stained with toluidine blue and used to localize areas with highest density of intranuclear inclusions. Resin blocks were trimmed accordingly, and ultrathin sections exhibiting silver interference were produced with diamond knives (Diatome, Biel, Switzerland) on a Reichert-Jung Ultracut E (Leica, Heerbrugg, Switzerland). Ultrathin sections were collected on collodion-coated 200 mesh copper grids (Electron Microscopy Sciences, Hatfield, PA). Sections were then double stained with 0.5% uranyl acetate for 30 minutes at 40°C (Sigma Aldrich, Steinheim, Germany) and 3% lead citrate for 10 minutes at 20°C (Leica, Heerbrugg, Switzerland) in an Ultrastain (Leica, Vienna, Austria) and examined in a Philips CM12 transmission electron microscope (FEI, Eindhoven, Holland) at an accelerating voltage of 80 kV. Micrographs were captured with a Mega View III camera using the iTEM software version 5.2 (Olympus Soft Imaging Solutions GmbH, Münster, Germany).

Virus Isolation

Portions of affected frog skin were finely homogenized and then ground in a mortar with quartz powder. The homogenized tissue was resuspended in cell culture medium (Ham's F12 K 50% with 40% sterile distilled water, 10% fetal bovine serum [FBS], 1% Pen/strep antibiotic mix, and 1% Amphotericin B) (Gibco by Thermofisher, Lucern, Switzerland). The homogenate was centrifuged at 800 × *g* for 10 minutes and the supernatant was split into 2 aliquots. One of the aliquots was filtered with a 0.45-µm filter, whereas the other was left unfiltered. The aliquots were then diluted 1/5 in complete cell culture medium as described above but with 5% ciprofloxacin (Bayer, Switzerland) and overlaid either on ICR-2A (Istituto Zooprofilattico Sperimentale della Lombardia e dell'Emilia, cell line repository) or *Terrapene* heart cell (TH1 Subline B1) (ATCC CCL50) monolayers, respectively. The cells were placed in an incubator at either 17°C (ICR-2A) or 25°C (ICR-2A and TH-1) for 2 hours, washed with phosphate-buffered saline (PBS), and incubated with fresh medium at the temperatures described above and monitored daily for cytopathic effects (CPEs) for 4 weeks.

Polymerase Chain Reaction (PCR) and Sequencing

Different PCR protocols were adopted to detect RHV3 genomic DNA. Initially, a consensus "panherpes" PCR protocol was selected.[37] Considering the possibility of an adenovirus infection also compatible with the location and partially with the

tinctorial affinity of the viral inclusions, a "panadenovirus" consensus PCR was also used.[38] Finally, an RHV3-specific PCR protocol targeting the partial sequence of the DNA polymerase gene was developed based on the preliminary sequences obtained. More specifically, 40 pmol each of forward (5′-TTATATTCAATTAGAGACCACC-3′) and reverse (5′- GCAGGATCGGGAGAATGG-3′) primers were added to a reaction mix composed of 3 µl of 10× reaction buffer, 0.4 µl of a 10 mM dNTPs mix, 5 units of Taq DNA polymerase (Qiagen, Hombrechtikon, Switzerland), and distilled deionized water to a final volume of 30 µl. The cycling reaction was carried out on an Applied Biosystems Thermocycler 9600 Fast (Applied Biosystems, Foster City, CA) and consisted of an initial denaturation step at 95°C for 3 minutes followed by 35 cycles comprising a 30-second denaturation step at 95°C, 30 seconds of annealing at 50°C, and an elongation step at 72°C for 30 seconds. A final elongation at 72°C for 10 minutes was carried out to exhaust the polymerase. The obtained amplicon was then resolved in a 1.5% agarose gel and examined under ultraviolet light.

For Sanger sequencing, the PCR amplicons were sequenced using the same primers as for their amplification with an automated sequencer (ABI Prism 3100 genetic analyzer; Applied Biosystems) using the BigDye Terminator cycle sequencing kit (Applied Biosystems) according to the manufacturer's instruction.

For next-generation sequencing (NGS), from the DNA extracted from skin samples containing a high density of intranuclear inclusions collected from the 2 diseased frogs, 3 µg of total DNA obtained by pooling was submitted to a private biotechnology company (Fasteris SA, Geneva, Switzerland) for NGS. The DNA template library was sequenced with the Illumina HiSeq 2500 to obtain 125 base long paired-end reads. De novo genome assembly was performed using the VELVET software (Version 1.3) (http://www.ebi.ac.uk/~zerbino/velvet/) as previously described.[26]

As a quality control step, the paired Illumina reads were mapped to the obtained genome sequence using Burrows-Wheeler transform;[17] the mapping was visualized with an Integrative Genomic Viewer 2.3.34.[35] The assembled sequence obtained was also mapped using Geneious software (V.91.5; http://www.geneious.com)[16] using the original NGS reads with standard setting and iterated 25 times. For open reading frame (ORF) identification, the software ORFfinder (https://www.ncbi.nlm.nih.gov/orffinder/) was used, and an arbitrary cutoff of at least 90 codons was selected. Each of the amino acid sequences encoded by the predicted ORF was analyzed by the Basic Local Alignment Search Tool (BLAST; http://blast.ncbi.nlm.nih.gov/Blast.cgi). All the predicted amino acid sequences that yielded no results with BLAST were examined with the software Phyre2 (http://www.sbg.bio.ic.ac.uk/~phyre2/html/page.cgi?id=index) for specific domain recognition and structural modeling.

Phylogenetic Analysis

The amino acid sequence of the DNA polymerase and that of the terminase proteins were selected for phylogenetic analysis given their high conservation among *Herpesvirales*. The amino acid sequences of the selected proteins from RHV3 were compared with the homologous protein sequences of other members of the family *Alloherpesviridae* from different genera. More specifically, the amino acid sequence of the DNA polymerase protein of RHV3 was compared with the homologous protein sequence encoded by 9 *Alloherpesviridae* (Genbank accession numbers: *Iactalurid HV1*-NP_041148.2; *Iactalurid HV2*-ACZ55873.1; *Acipenserid HV2*-ACZ55868.2; *Ranid HV2*-ABG25576.1; *Ranid HV1*-YP_656727.1; *Anguillid HV1*-ADQ54121.1; *Cyprinid HV1*-AAX53084.1; *Cyprinid HV2*-YP_007003898.1; *Cyprinid HV3*-AAX53082.1), whereas 7 sequences were used for the phylogenetic analysis of the terminase protein (Genbank accession numbers: *Iactalurid HV1*-NP_041153.2; *Ranid HV1*-YP_656697.1; *Ranid HV2*-YP_656576.1; *Anguillid HV1*-YP_003358149.1; *Cyprinid HV1*-YP_007003702.1; *Cyprinid HV2*-YP_007003857; *Cyprinid HV3*-YP_001096069.2). The sequences of the DNA polymerase and of the terminase proteins of *Testudinid herpesvirus 3* (TeHV3) strain US1976/98, an Alphaherpesvirus, were used as outgroup for the phylogenetic analyses (UL30 [Genbank accession number AKV40702.1] for the DNA polymerase and UL15A-UL15B [Genbank accession numbers AKV40686.1 and AKV40689.1] for the terminase analysis, respectively). The sequences of the 3 putative exons of RHV3 showing similarity with the terminase amino acid sequence were concatenated for the phylogenetic analysis similarly to the 2 putative exons of the TeHV3 terminase protein. The amino acid sequences were aligned with ClustalW (SDS-Biological workbench; http://workbench.sdsc.edu), and a consensus maximum likelihood phylogenetic tree was constructed using the software Mega 6.0-6[33] with the standard settings and 500 bootstrap replications, the Jones Taylor Thornton (JTT) replication method, uniform rates among sites, and a very strong branch swap filter.

The genomes of RHV1 (Genbank accession number NC_008211), RHV2 (Genbank accession number NC_008210), and RHV3 (Genbank accession number KX832224) were compared using the software Easyfig 2.1 using standard settings.[32]

Results

Gross Pathology

The 2 frogs examined both had severe proliferative skin lesions characterized by prominent, multifocal, poorly demarcated light tan to gray, slightly raised, firm skin patches ranging from 1 to 3 mm diameter (Fig. 1). These lesions extended over the dorsal and ventral aspects of the body but more severely affected the dorsum, both flanks, and the dorsal aspect of the thighs. Furthermore, on the ventrum, the lesions extended from the base of the neck to the caudal abdomen. Additional gross findings included intestinal nematodes in one frog and lung nematodes *(Rhabdias spp)* in the other.

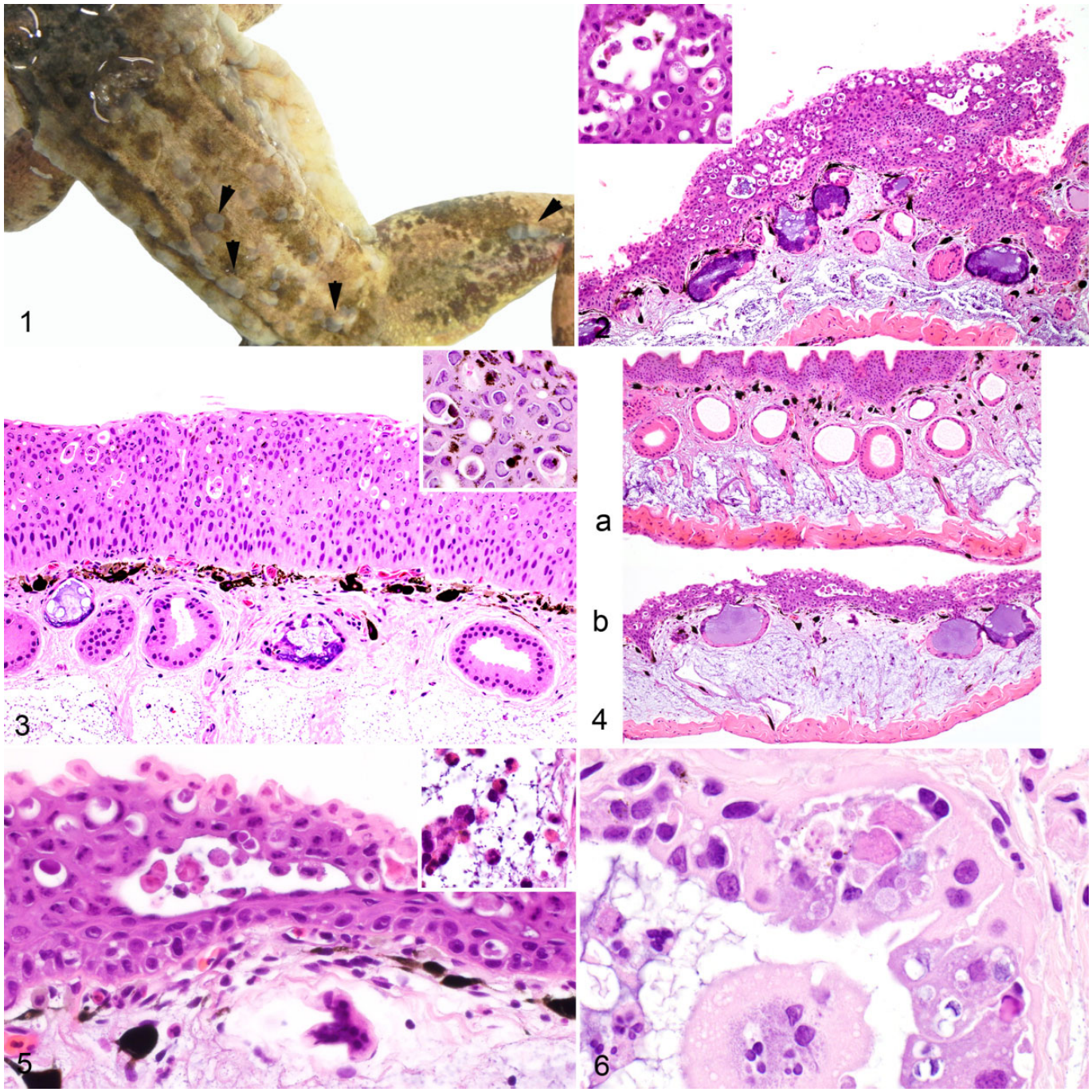

Figures 1–6. Ranid herpesvirus 3 (RHV3)–associated epidermal hyperplasia, common frog (*Rana temporaria*). **Figure 1.** Multifocal to coalescent light tan to gray patches of skin are present, more frequently on the dorsum and along the flanks (black arrows). **Figure 2.** The gray areas observed grossly correspond to areas of epidermal hyperplasia with intercellular clear spaces (inset) and dermal edema. Glands have an irregular profile and some appear compressed or collapsed. Hematoxylin and eosin (HE). **Figure 3.** The epidermal layer is severely thickened and contains large numbers of intranuclear amphophilic inclusions (inset). Clusters of necrotic keratinocytes with karyorrhexic and pyknotic nuclei are present in areas with many inclusions. Glands have variable epithelial hyperplasia (HE). **Figure 4.** (a) Unaffected and (b) affected skin. The affected skin shows prominent edema throughout the stratum spongiosum of the dermis. HE. **Figure 5.** In areas with epidermal hyperplasia, the dermis is infiltrated by only a few inflammatory cells, including lymphocytes, monocytes, and heterophils. Inset: heterophils in the edematous dermis. HE. **Figure 6.** A mucous gland shows severe epithelial cell degeneration with prominent vacuolization and hypereosinophilic granular cytoplasm. The gland lumen contains a large degenerating cell and few heterophils. HE.

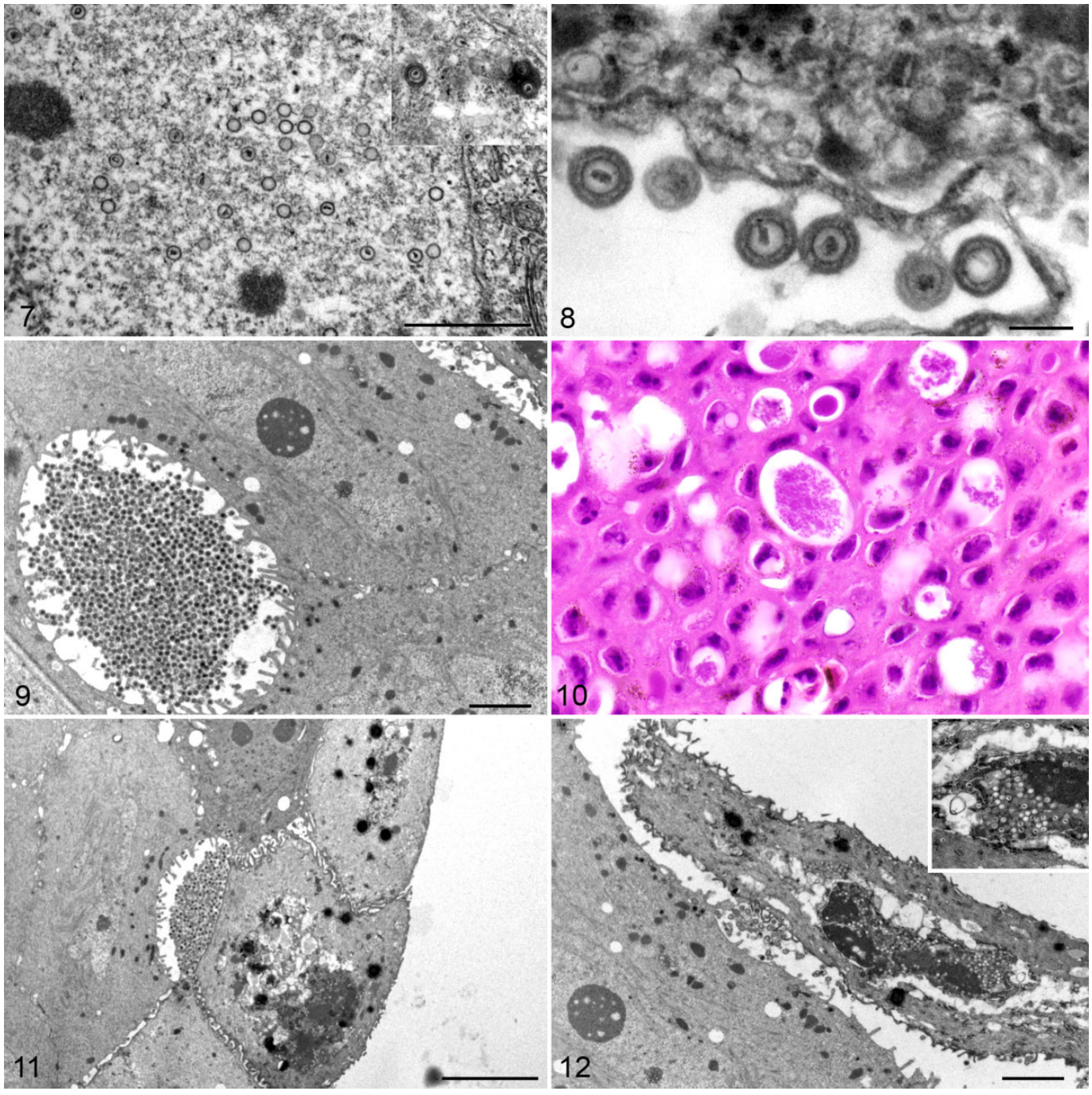

Figures 7–12. Ranid herpesvirus 3 (RHV3) ultrastructural features, skin, common frog (*Rana temporaria*). **Figure 7.** Viral particles with icosahedral symmetry and frequently containing an electron-dense core are in the nucleus of an epidermal cell. Inset: Capsids outside the nucleus are surrounded by a tegument and a membrane (envelope). Scale bar = 1 μm. Transmission electron microscopy (TEM). **Figure 8.** Several budding viral particles are attached to the cell with a peduncular stalk. Scale bar = 200 nm. TEM. **Figure 9.** Unique clustering of large numbers of viral particles within the intercellular space. Scale bar = 2 μm. TEM. **Figure 10**. The viral particles shown in Fig. 9 correspond to the granular material observed by light microscopy. Hematoxylin and eosin. **Figure 11.** A necrotic epidermal cell is detaching from the epidermis with a subjacent pocket full of viral particles. Scale bar = 5 μm. TEM. **Figure 12.** A completely detached epidermal cell contains large numbers of viral particles (inset). Scale bar = 2 μm. TEM.

Histopathology

The proliferative skin lesions observed grossly corresponded to multifocal plaque-like regions of epidermal hyperplasia up to ≥3 times normal thickness (Figs. 2 and 3). The thickened epidermis showed prominent, variably extensive, multifocal intercellular clear spaces expanding in the upper layers where plump and rounded keratinocytes were accumulating (Fig. 2,

inset). In the more severely affected areas, these spaces were wider, more numerous, and extended to the deeper layers of the epidermis (Fig. 2). Frequently, dense to loose clusters of dark eosinophilic granular material, whose single elements were less than 0.5-μm diameter, were present in some of the smaller extracellular clear spaces (Fig. 2, inset). A large number of lightly eosinophilic to amphophilic intranuclear inclusions that marginated the chromatin were frequently observed in the hyperplastic areas of the epidermis (Fig. 3). Corresponding to areas with many inclusions, clusters of keratinocytes were necrotic with loss of cell detail and karyorrhexic and pyknotic nuclei (Fig. 3). The most affected areas had increased numbers of melanin-laden cells scattered within the epidermis. Spongiosis was also present but mostly circumscribed to the lower layers of the epidermis. The affected areas did not show hyperkeratosis. However, occasional mild parakeratosis was observed in the areas not undergoing hyperplasia. Multifocally, prominent dermal edema separated collagen fibers of the stratum spongiosum by clear space in the most severely affected epidermal sections, although not consistently (Fig. 4). Low numbers of lymphocytes, plasma cells, and few heterophils occasionally infiltrated the dermis (stratum spongiosum), rarely the epidermis (Fig. 5), and once a degenerate gland. The mucous glands in severely affected skin were inconsistently distorted, asymmetric, occasionally hyperplastic, and frequently had epithelial cell degeneration with cytoplasmic vacuolization and accumulation of degenerating and necrotic cells in the clear spaces opening into the epithelial wall. Degenerating cells collected in the lumina of some of the affected glands along with a few heterophils (Figs. 2–4, 6). Serous glands were not affected. A nematode larva was present in the lumen of 1 mucous gland.

Transmission Electron Microscopy

The nuclei of the epidermal cells contained large numbers of round, naked particles that were approximately 80-nm diameter and often had an electron-dense core surrounded by an icosahedral wall consistent with the condensed nucleic acid and the viral capsid, respectively (Fig. 7 and inset). Several particles appeared as empty capsids without electron-dense cores. Similar particles further surrounded by electron-dense elements consistent with the classic herpesviral tegument and envelope were observed in the cytoplasm of the infected cells, either free or embedded in an amorphous electron-dense matrix (Fig. 7, inset). The enveloped particles ranged from 180 to 190 nm in diameter. Furthermore, particles were observed budding from the cell membranes, and some remained bound to the host cell by thin stalks resembling pedunculated elements (Fig. 8). Dense clusters of viral particles accumulated in the extracellular clear spaces corresponded to the granular dark eosinophilic material seen by light microscopy in the HE-stained sections (Figs. 9 and 10). Finally, sloughed epithelial cells mainly associated with either extracellular (Fig. 11) or intracellular (Fig. 12) aggregates of viral particles were observed in the examined sections.

Polymerase Chain Reaction and Sequencing

The panherpesvirus consensus PCR[37] did not yield any detectable amplicon from any of the examined skin samples. The presence of intranuclear inclusions, although slightly eosinophilic to amphophilic, suggested the possibility of an adenovirus, and consequently a panadenovirus consensus PCR was also used[38] and yielded an amplicon of approximately 320 bp. The sequencing of the amplicon carried out with the Forward primer did not yield a readable result, whereas the Reverse primer sequencing yielded a 264-nt-long readable sequence, and analysis with the BLAST X program showed a single match to the viral DNA polymerase encoded by the ORF110 of RHV2 (Genbank YP_656618.1; 30% identity, 51% positive amino acid residues over a 76 amino acid portion, E identity value of 0.056). The ad hoc PCR primers designed on the obtained DNA sequence yielded an amplicon of 254 bp from both frog skin samples with proliferative lesions. PCR tests with the specific RHV3 primers (described above) carried out on the other tissues collected from the examined frogs were negative.

Characterization of the Ranid Herpesvirus 3 Genome

Next-generation sequencing of DNA extracted from skin lesions yielded a total of 10,956 Mbases obtained with 43.8 Mclusters, and 84.14% of the bases had a q-score larger than 30. The de novo assembly of the reads that was carried out with Velvet (http://www.ebi.ac.uk/~zerbino/velvet/) yielded a total of 131 scaffolds that spanned from 229 to 203,958 nt long for a total of 285,378 bases and an average scaffold length of 2,178 nt. The partial sequence of the DNA polymerase gene amplified by PCR was identified in the largest scaffold measuring 203,958 bases. This scaffold was then presumptively identified as part of the RHV3 genome and selected for further investigation. Geneious (V.91.5; http://www.geneious.com)[16] was then used to perform a 25-times iterated remapping of the reads using the selected scaffold as a reference. Following iteration, a unique consensus sequence 207,914 bases long was obtained. The 3′ end of the consensus sequence was flanked by a region identical to its putative 5′ end, whereas the sequence flanking the 5′ end of the 207-Kb consensus sequence was identical to its 3′ end, suggesting a circular nature of the molecule or the presence of a concatemer. Each base had at least 700 times coverage. The GC content was 41.82%. We were unable to identify the presence of terminal direct repeats similar to what is known for RHV1 and RHV2;[11] however, this does not rule out their presence in the genome.

RHV3 Genome Features

The RHV3 genome was determined to be 207,914 nt long. It contained 189 ORFs encoding for at least 90 codons. Their predicted sizes ranged from 270 (ORF74A) to 13,902 (RHV3-ORF86) nucleotides (Suppl. Table S1). At least 41 of the predicted proteins encoded by the detected ORFs had

similarities with proteins encoded by the RHV1 and/or RHV2 genomes (Suppl. Table S1). The highest similarity was observed for ORF100 encoding for part of the terminase protein (65% similarity with RHV1-ORF53). The lowest similarity was that of RHV3-ORF16, which shares 36% similarity with ORF26 of RHV2 (Suppl. Table S1). Co-linearity between the gene arrangement of RHV3 and that of the RHV1 and RHV2 is evident in the RHV3 genome spanning between ORF66 and 135. All 12 genes conserved across all known *Alloherpesviruses* (RHV3-ORF56, 57, 62, 64, 65, 72, 74, 75, 80, 88, 90, and the putative terminase exons [53, 100 102]) were identified in the RHV3 genome (Suppl. Table S1) together with the 13th gene present in all the known *Alloherpesviruses* with the exception of *Anguillid herpesvirus* 1 (RHV3-ORF97 and 98).[2,12]

Of interest is the presence of ORFs predicted to encode proteins not observed in RHV1 or RHV2 or in other *Alloherpesviruses,* such as ORF30 encoding for a protein of the B22 family observed up to now only in poxviruses with potent immunosuppressive activity against T cells.[1] A gene encoding for a protein sharing predicted similarity with FOXM1 (ORF36), a critical factor in regulating the cell cycle, was also identified (Suppl. Table S1).[9] Finally, at least 2 clusters of ORFs encoding predicted C-type lectin proteins were identified in the RHV3 genome, with one of them (ORF132) encoding a protein predicted to share strong (99.9%) structural similarities with the Epstein-Barr virus ligand gp42 (Suppl. Table S1). All the NGS reads mapping to the "unique" RHV3 genes were bridging at high coverage with the genomic regions contiguous to the 5′ and 3′ ends of these genes similarly to the RHV3 homologous genes to RHV1 and RHV2.

Of the other 130 scaffolds obtained by NGS, 4 scaffolds were determined to map within the 207-Kb predicted genome, whereas 86 scaffolds were identified as portions of genes from amphibians or other nonviral organisms. The remaining 40 scaffolds yielded no known matches via BLASTX either by general search or by focusing on *"Amphibia"* or *"Viruses"* taxa.

Phylogenetic Analysis and Genome Comparison

Phylogenetic analysis of the DNA polymerase and the terminase yielded maximum likelihood phylogenetic trees with overlapping topology and unambiguous clustering of RHV3 into the *Batrachovirus* genus of the family *Alloherpesviridae*. Furthermore, RHV3 appears to be more closely related to RHV1 than to RHV2, consistent with the results of the genome analysis (Figs. 14 and 15).

Comparison of the RHV3 genome with those of RHV1 and RHV2 carried out with Easyfig[32] showed clustering of the highest predicted similarities within the central portion of the genomes where the bulk of the conserved and co-linear genes shared by the 3 ranid herpesviruses are located. The highest similarities were observed between RHV3 and RHV1 (Fig. 13).

Figure 13. The genome structures of ranid herpesviruses 1, 2, and 3 (RHV1, RHV2, RHV3) are compared. The numbers labeling the genomes at their left end in the image refer to the specific viral species (1 = RHV1; 2 = RHV2, 3 = RHV3). Connector lines link conserved homologous genes from the different genomes. The most conserved genes are clustered within the central portions of the genomes (blue rectangle). The intensity of the color of the connector lines (gray) is directly proportional to the degree of conservation of the homologous genes (the figure was obtained with the software Easyfig 2.1).

Virus Isolation

No cytopathic effects and no virus could be detected in the cell cultures at 1 month from the initial seeding of the inoculum and after 4 blind passages.

Discussion

In this article we report the identification, partial characterization, associated pathology, and genome sequencing of a newly identified herpesvirus with convincing molecular features supporting its position in the genus *Batrachovirus* in the family *Alloherpesviridae* and tentatively named *Ranid herpesvirus 3* (RHV3). The first major feature in the RHV3-infected frogs was a proliferative change similar to that observed in other herpesvirus-associated diseases, including that caused by RHV1.[19,20,22] Interestingly, RHV3 appears to be more closely related to RHV1 than RHV2, and RHV3-ORF36 encodes a protein that shares 60% structural similarity with the Forkhead box protein M1 (FOXM1), a protein known to be involved in the regulation of the cell cycle and overexpressed in several carcinomas.[9]

The second major feature of the lesions associated with RHV3 is the presence of prominent lightly eosinophilic to amphophilic intranuclear inclusions with marginalization of the chromatin, often associated with cellular necrosis in the affected tissues, similar to other herpesviruses.[26]

The third major feature associated with RHV3 infection is the presence of granular eosinophilic aggregates within variably extensive clear spaces of the thickened skin. Electron microscopy revealed that the granular aggregates were myriads of mature viral particles collecting in extracellular spaces that resulted from the dissociation of adjacent keratinocytes. Accumulations of such dense clusters of virions in extracellular spaces have never been reported for other herpesviruses, to the

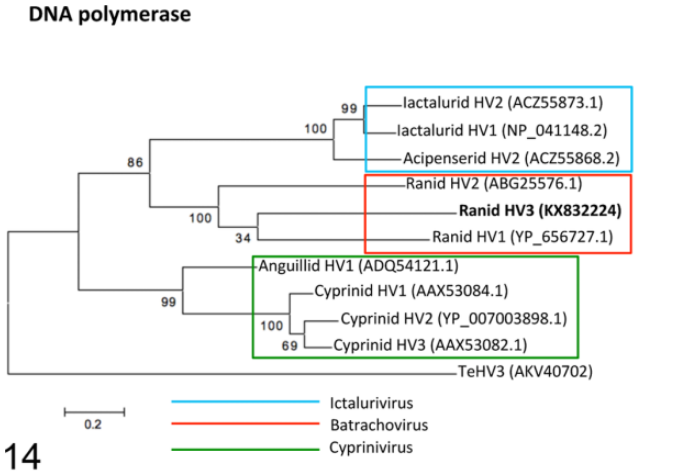

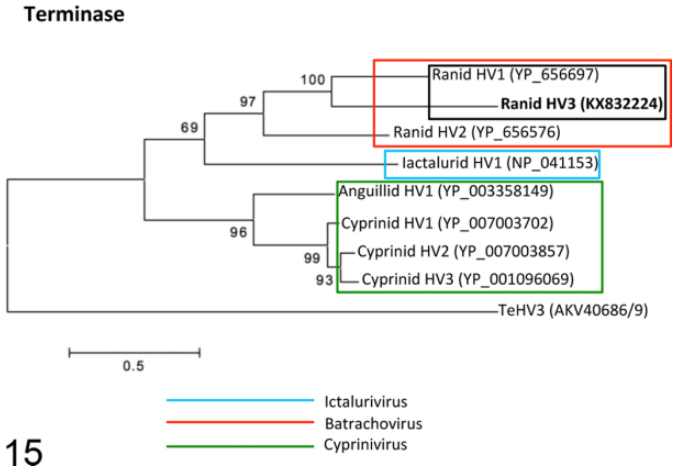

Figures 14–15. The maximum likelihood trees based on the DNA polymerase (Fig. 14) and terminase (Fig. 15) amino acid sequences show clustering of *Ranid herpesvirus* 3 (RHV3) with the homologous proteins from other members of the genus *Batrachovirus*. RHV3 appears to be phylogenetically closer to RHV1 than to RHV2. The amino acid sequence of the *Testudinid herpesvirus 3* (TeHV3) DNA polymerase and terminase have been used as the outgroups for the analyses. Genbank accession numbers are indicated in parentheses.

best of our knowledge, and may be a unique feature of RHV3, possibly being relevant for virus transmission.

Skin lesions were associated with a minimal inflammatory response. This may reflect either the compromised status of the immune system a few weeks out of hibernation, as is known in poikilotherms, or an immunomodulatory effect of the virus.[8,25,26] Interestingly, RHV3-ORF30 is predicted to encode a protein with similarity to protein encoded by the B22 gene family, a group of genes detected in poxviruses and recently shown to be associated with a temporary "T-cell paralysis."[1]

The lesions observed in the RHV3-infected frogs closely resemble those previously reported in other frogs and attributed to uncharacterized herpesviruses.[3,14,15] A herpesvirus-associated proliferative skin disease was identified in *R. dalmatina* in Italy in 1994,[3] and an RHV3-specific PCR assay carried out on formalin-fixed, paraffin-embedded tissue from this case yielded a detectable amplicon using the same set of primers reported above. The nucleotide sequence obtained from the paraffin block showed 97% identity with the homologous sequence obtained from the RHV3-infected frogs investigated in this study (data not shown). This suggests that the herpesvirus strains that infected R. dalmatina in Italy in 1994 and R. temporaria in Switzerland in 2015 are very closely related viruses. A broader retrospective investigation is needed to better understand the epidemiology of RHV3 and its relevance for conservation.

The genome of RHV3 appears to be shorter than the genomes of RHV1 and RHV2, and it has a relatively low GC content (41.82%) compared with RHV1 (54.6%), RHV2 (52.8%), and other alloherpesviruses.[36] At least 41 genes of the RHV3 genome encoded proteins showing similarities to the homologous gene products of RHV1 and RHV2. The arrangement of the conserved genes among the 3 ranid herpesviruses is also well conserved, with the bulk of them clustering within the central region of the genome in RHV3, similar to RHV1, RHV2, and other herpesviruses[26] and indirectly supporting the accuracy of the genome assembly.

In conclusion, this study describes the first detection of RHV3, a proposed new member of the genus *Batrachovirus* in the family *Alloherpesviridae*. The virus was associated with a clinically relevant proliferative skin disease characterized by severe multifocal epidermal hyperplasia, intranuclear inclusions, dermal edema, and variable degeneration of the mucous glands. A unique ultrastructural feature of the RHV3-associated infection was the presence of dense clusters of mature virions in the extracellular spaces, possibly relevant for virus transmission. Finally, the genome of RHV3 contains all of the most conserved genes across the alloherpesviruses and has a gene arrangement very similar to the gene arrangements of the other known ranid herpesviruses. These findings are relevant to understanding the biology of the members of the family *Alloherpesviridae* and the role of these pathogens in the global decline of amphibians, the most endangered vertebrate group on earth.

Acknowledgements

We thank Drs Maura Ferrari and Antonio Lavazza from the Istituto Zooprofilattico Sperimentale della Lombardia e dell'Emilia (IZSLER) (Italy) for the kind gift of the ICR-2A cell line and all the FIWI personnel for the technical assistance. We also thank Drs Lucia Gibelli and Antonio Lavazza (IZSLER) (Italy) for providing a tissue block from the 1994 herpesvirus associated outbreak in *Rana dalmatina*. Finally, we thank Dr Helmut Segner for a critical review of the manuscript and Dr Ian Hawkins for further insights and English editing.

Declaration of Conflicting Interests

The author(s) declared no potential conflicts of interest with respect to the research, authorship, and/or publication of this article.

Funding

The author(s) disclosed receipt of the following financial support for the research, authorship, and/or publication of this article: This study was made possible thanks to the grant no. 2013-11-18/206 from the Swiss Federal Veterinary Office (BLV) for the "Support of early

detection of contagious diseases in wildlife" and internal departmental funding including that provided by the Division of Veterinary Anatomy, University of Bern, and the department of Evolutionary Biology and Environmental Studies, University of Zurich.

References

1. Alzhanova D, Hammarlund E, Reed J, et al. T cell inactivation by poxviral B22 family proteins increases viral virulence. *PLoS Pathog*. 2014;**10**(5):e1004123.
2. Aoki T, Hirono I, Kurokawa K, et al. Genome sequences of three koi herpesvirus isolates representing the expanding distribution of an emerging disease threatening koi and common carp worldwide. *J Virol*. 2007;**81**(10):5058–5065.
3. Bennati R, Bonetti M, Lavazza A, et al. Skin lesions associated with herpesvirus-like particles in frogs (*Rana dalmatina*). *Vet Rec*. 1994;**135**(26):625–626.
4. Berger L, Speare R, Dazsak P, et al. Chytridiomycosis causes amphibian mortality associated with population declines in the rain forests of Australia and Central America. *Proc Natl Acad Sci U S A*. 1998;**95**(15):9031–9036.
5. Breidenbach GP, Skinner MS, Wallace JH, et al. In vitro induction of a herpes-type virus in "summer-phase" Lucké tumor explants. *J Virol*. 1971;**7**(5):679–682.
6. Catenazzi A. State of the world's amphibians. *Ann Rev Envir Res*. 2015;**40**:91–119.
7. Collins JP, Storfer A. Global amphibian declines: sorting the hypotheses. *Divers Distrib*. 2003;**9**:89–98.
8. Cooper EL, Wright RK, Klempau AE, et al. Hibernation alters the frog's immune system. *Cryobiology*. 1992;**29**(5):616–631.
9. Dai J, Yang L, Wang J, et al. Prognostic value of FOXM1 in patients with malignant solid tumor: a meta-analysis and system review [published online July 22, 2015]. *Dis Markers*. doi:10.1155/2015/352478.
10. Daszak P, Cunningham AA, Hyatt AD. Infectious disease and amphibian population declines. *Divers Distrib*. 2003;**9**:141–150.
11. Davison AJ, Cunningham C, Sauerbier W, et al. Genome sequences of two frog herpesviruses. *J Gen Virol*. 2006;**87**(pt 12):3509–3514.
12. Davison AJ, Kurobe T, Gatherer D, et al. Comparative genomics of carp herpesviruses. *J Virol*. 2013;**87**(5):2908–2922.
13. Duffus ALJ, Cunningham AA. Major disease threats to European amphibians. *Herpetol J*. 2010;**20**(3):117−127.
14. Garner TWJ, Martel A, Bielby J, et al.Chapter 31: Infectious diseases that may threaten Europe's amphibians. In: Heatwole H, Wilkinson JW, eds. *Amphibian Biology*, Vol **11**. Exeter, UK: Pelagic Publishing; 2013:1–41.
15. Grossenbacher K. Eine Springfroschkrankheit auf der Alpensuedseite. *RANA*. 1997;**2**:203–205.
16. Kearse M, Moir R, Wilson A, et al. 2012. Geneious basic: an integrated and extendable desktop software platform for the organization and analysis of sequence data. *Bioinformatics*. 2012; **28**(12):1647–1649.
17. Li H, Durbin R. Fast and accurate short read alignment with Burrows-Wheeler transform. *Bioinformatics*. 2009;**25**(5):1754–1760.
18. Lips KR, Brem F, Brenes R, et al. Emerging infectious disease and the loss of biodiversity in a neotropical amphibian community. *Proc Natl Acad Sci U S A*. 2006;**103**(9):3165–3170.
19. Lucke B. Carcinoma in the leopard frog: its probable causation by a virus. *J Exp Med*. 1938;**68**(4):457–468.
20. Lucke B. A neoplastic disease of the kidney of the frog. Rana pipiens. *Am J Cancer*. 1934;**20**:352–379.
21. Martel A, Spitzen-van der Sluijs A, Blooi M, et al. *Batrachochytrium salamandrivorans* sp. nov. causes lethal chytridiomycosis in amphibians. *Proc Natl Acad Sci U S A*. 2013;**110**(38):15325–15329.
22. McKinnell RG. The Lucké frog kidney tumor and its herpesvirus *American Zoologist*. 1973;**13**(1):97–114.
23. McKinnell RG, Tarin D. Temperature-dependent metastasis of the Lucke renal carcinoma and its significance for studies on mechanisms of metastasis. *Cancer Metastasis Rev*. 1984;**3**(4):373–386.
24. Mutschmann F, Schneeweiss D. Herpes-Virus-Infektionen bei *Pelobates fuscus* und anderen Anuren im Berlin-Brandenburger Raum. *Rana*. 2008; **5**:113–118.
25. Origgi F. Reptile immunity. In: Jacobson ER, ed. *Infectious Diseases and Pathology of Reptiles*. Boca Raton, FL: CRC Press; 2007:131–166.
26. Origgi FC, Tecilla M, Pilo P, et al. A genomic approach to unravel host-pathogen interaction in chelonians: the example of Testudinid herpesvirus 3. *PLoS One*. 2015;**10**(8):e0134897.
27. Price SJ, Garner TW, Nichols RA, et al. Collapse of amphibian communities due to an introduced Ranavirus. *Curr Biol*. 2014;**24**(21):2586–2591.
28. Rafferty KA Jr. The biology of spontaneous renal carcinoma of the frog. In: King JS, ed. *Renal Neoplasia*. Boston, MA: Little, Brown; 1967:311–315.
29. Rafferty KA Jr. The cultivation of inclusion-associated viruses from Lucké tumor frogs. *Ann N Y Acad Sci*. 1965;**126**(1):3–21.
30. Rodriguez-Ramos Fernandez J, Franklinos L, Everest D, et al. Ranid herpesvirus skin disease in common frogs (*Rana temporaria*) in Great Britain. Paper presented at: 12th Conference of the European Wildlife Disease Association (EWDA); August 27–31, 2016; Berlin, Germany.
31. Skerratt LF, Berger L, Speare R, et al. Spread of chytridiomycosis has caused the rapid global decline and extinction of frogs. *EcoHealth*. 2007; **4**:125–134.
32. Sullivan MJ, Petty NK, Beatson SA. Easyfig: a genome comparison visualiser. *Bioinformatics*. 2011;**27**(7):1009–1010.
33. Tamura K, Stecher G, Peterson D, et al. MEGA6: Molecular Evolutionary Genetics Analysis version 6.0. *Mol Biol Evol*. 2013;**30**(12):2725–2729.
34. Teacher AGF, Cunningham AA, Garner TWJ. Assessing the long-term impact of Ranavirus infection in wild common frog populations. *Anim Conservation*. 2010;**13**(2010):514–522.
35. Thorvaldsdóttir H, Robinson JT, Mesirov JP. Integrative Genomics Viewer (IGV): high-performance genomics data visualization and exploration. *Brief Bioinform*. 2013;**14**(2):178–192.
36. van Beurden SJ, Bossers A, Voorbergen-Laarman MH, et al. Complete genome sequence and taxonomic position of Anguillid herpesvirus 1. *J Gen Virol*. 2010; **91**(pt 4):880–887.
37. VanDevanter DR, Warrener P, Bennett L, et al. Detection and analysis of diverse herpesviral species by consensus primer PCR. *J Clin Microbiol*. 1996;**34**(7):1666–1671.
38. Wellehan JF, Johnson AJ, Harrach B, et al. Detection and analysis of six lizard adenoviruses by consensus primer PCR provides further evidence of a reptilian origin for the atadenoviruses. *J Virol*. 2004;**78**(23):13366–13369.